Title

Human Eukaryotic Initiation Factor 2 (eIF2)-GTP-Met-tRNAi Ternary Complex and eIF3 Stabilize the 43 S Preinitiation Complex*

Journal

Journal of Biological Chemistry, 289(46)

ISSN

0021-9258

Authors

Sokabe, Masaaki

Fraser, Christopher S

Publication Date

2014-11-01

DOI

10.1074/jbc.m114.602870

THE JOURNAL OF BIOLOGICAL CHEMISTRY VOL. 289, NO. 46, pp. 31827–31836, November 14, 2014

Human Eukaryotic Initiation Factor 2 (eIF2)-GTP-Met-tRNA$_i$ Ternary Complex and eIF3 Stabilize the 43 S Preinitiation Complex*

Received for publication, August 4, 2014, and in revised form, September 15, 2014 Published, JBC Papers in Press, September 22, 2014, DOI 10.1074/jbc.M114.602870

Masaaki Sokabe and Christopher S. Fraser[1]

From the Department of Molecular and Cellular Biology, College of Biological Sciences, University of California, Davis, California 95616

Background: 43 S preinitiation complex (PIC) formation is an important step for eukaryotic translation initiation.
Results: A thermodynamic framework of human 43 S PIC reveals a complicated network of positive and negative cooperativity among the components.
Conclusion: eIF2 and eIF3 play essential roles in stabilizing the 43 S PIC.
Significance: Quantitative analysis of initiation complex formation leads to understanding of mechanistic details in translation initiation.

The formation of a stable 43 S preinitiation complex (PIC) must occur to enable successful mRNA recruitment. However, the contributions of eIF1, eIF1A, eIF3, and the eIF2-GTP-Met-tRNA$_i$ ternary complex (TC) in stabilizing the 43 S PIC are poorly defined. We have reconstituted the human 43 S PIC and used fluorescence anisotropy to systematically measure the affinity of eIF1, eIF1A, and eIF3j in the presence of different combinations of 43 S PIC components. Our data reveal a complicated network of interactions that result in high affinity binding of all 43 S PIC components with the 40 S subunit. Human eIF1 and eIF1A bind cooperatively to the 40 S subunit, revealing an evolutionarily conserved interaction. Negative cooperativity is observed between the binding of eIF3j and the binding of eIF1, eIF1A, and TC with the 40 S subunit. To overcome this, eIF3 dramatically increases the affinity of eIF1 and eIF3j for the 40 S subunit. Recruitment of TC also increases the affinity of eIF1 for the 40 S subunit, but this interaction has an important indirect role in increasing the affinity of eIF1A for the 40 S subunit. Together, our data provide a more complete thermodynamic framework of the human 43 S PIC and reveal important interactions between its components to maintain its stability.

In the current model of eukaryotic translation initiation, a stable 43 S preinitiation complex (PIC)[2] must be formed prior to mRNA recruitment (1, 2). The initiator Met-tRNA$_i$ that encodes the first amino acid is recruited to the 40 S ribosomal subunit as a ternary complex (TC) with eIF2 and GTP. This step is facilitated by initiation factors eIF1, eIF1A, eIF3, and eIF5, which together form the 43 S PIC. The 43 S PIC is recruited to a 5′ end of an mRNA in a step that requires cap recognition by the eIF4F complex. Following recruitment, the 40 S subunit migrates along the mRNA until it reaches an initiation codon where the 60 S subunit joins to form the 80 S initiation complex.

Many studies over the years have investigated the interactions between the components that constitute the 43 S PIC both *in vitro* and *in vivo* (3). The interaction between initiation components and the 40 S subunit have generally been followed by non-equilibrium methods such as sucrose gradient centrifugation, size exclusion chromatography, and gel-shift assays. The analysis of 40 S complexes by sucrose gradient analysis often results in the dissociation of eIF1, eIF1A, and eIF3 (4–6). The integrity of these labile complexes can be maintained by the use of cross-linking agents, but this makes it difficult to quantitatively interpret how different factors function in complex stability. Analysis of 40 S complexes by size exclusion chromatography has been shown to improve the integrity of some 40 S complexes. In particular, this approach has been able to show that eIF1, eIF1A, and eIF3 help stabilize the TC on the 40 S subunit (6). Similar to size exclusion chromatography, gel-shift assays are able to detect some 40 S complexes that cannot withstand sucrose gradient analysis (7, 8). Although these techniques can provide information regarding the relative stability of different complexes, dissociation of complexes often occurs because the samples are not at equilibrium. Moreover, an inability to observe a stabilizing effect between two components using these non-equilibrium techniques cannot be interpreted to mean that they do not in fact stabilize each other's binding to the 40 S subunit. As a result, non-equilibrium techniques make it difficult to determine the affinities of interactions between components.

Work using sophisticated biochemical analysis of yeast eIF1 and eIF1A has revealed thermodynamic and kinetic details of how these factors bind the 40 S subunit in a cooperative manner, and how they ensure correct start codon recognition (9–16). Importantly, yeast eIF1 and eIF1A are thermodynamically coupled with TC binding to the 40 S subunit in the absence and presence of mRNA (9, 13, 17–19). Additionally,

* This work was supported, in whole or in part, by National Institutes of Health Grant RO1 GM092927 (to C. S. F.). This work was also supported by Japan Society for the Promotion of Science (JSPS) Postdoctoral Fellowships for Research Abroad (to M. S.).
[1] To whom correspondence should be addressed. Tel.: 530-752-1716; Fax.: 530-752-3085; E-mail: csfraser@ucdavis.edu.
[2] The abbreviations used are: PIC, preinitiation complex; TC, ternary complex; GMPPNP, 5′-guanylyl imidodiphosphate.

eIF1 and eIF1A also interact with eIF5 to ensure correct start codon recognition (11, 15, 18). Yeast and human eIF3 interacts directly with eIF1, TC, and eIF5 to form a multifactor complex in yeast, plants, and mammals (8, 20, 21). Accordingly, mutations in eIF3 subunits lower the apparent affinity of eIF1, eIF1A, eIF5, and TC for the 40 S *in vivo* (reviewed in Refs. 3 and 22). However, because eIF1, eIF1A, and TC are able to bind to the 40 S subunit with high affinity in the absence of eIF3, it is unclear why eIF3 is so important for the stability of the 43 S PIC (8, 11). To date, no quantitative assays have been used to determine how eIF3 interacts with eIF1, eIF1A, and TC in the 43 S PIC. It is well documented that eIF1, eIF1A, and the TC all bind on the 40 S subunit interface either in or close to the mRNA decoding site, which is fundamental for their proposed function in mRNA recruitment and initiation codon selection (23–29). In contrast, the only eIF3 subunit that has been shown to bind to the decoding site of the 40 S subunit is eIF3j (30). Human and yeast eIF3j both increase the affinity of the eIF3 complex for the 40 S subunit, as determined by sucrose gradient centrifugation (31, 32). Surprisingly, the binding of eIF3j to the 40 S subunit substantially weakens the affinity of eIF1A for the 40 S subunit and actually inhibits mRNA recruitment, albeit in a complex that does not include eIF3 (30). Taken together, it is clear that eIF3, eIF1, eIF1A, and the TC all interact with one another and the 40 S subunit to form the 43 S PIC, but the thermodynamic and kinetic frameworks for these interactions need to be determined to fully understand how this complex is formed prior to mRNA recruitment.

Here, we have used a highly purified reconstituted human system to explore how eIF1, eIF1A, eIF3, and TC components affect each other's affinity for the 40 S subunit. We will refer to this complex throughout this study as the 43 S PIC although it is formed in the absence of eIF5 (see "Discussion"). Using a steady state anisotropy assay, we have measured the affinity of fluorescently labeled eIF1, eIF1A, and eIF3j for the 40 S subunit in the presence of different combinations of 43 S PIC components. Our data demonstrate that the positive cooperativity between eIF1 and eIF1A binding to the 40 S subunit is conserved through evolution. Moreover, this cooperativity is important in enabling the TC and eIF3 to interact with both eIF1 and eIF1A to ensure the stability of the 43 S PIC.

EXPERIMENTAL PROCEDURES

Sample Preparation—Endogenous human eIF2 and 40 S ribosomal subunits were purified from HeLa cell extracts as described previously (30). Endogenous eIF3 lacking the j subunit (eIF3Δj) also was prepared from HeLa cell extracts through gel filtration chromatography under high salt conditions as described previously (30). Initiator tRNA was *in vitro* transcribed with T7 RNA polymerase and methionylated by *Escherichia coli* methionyl-tRNA synthetase as described previously (30). Recombinant wild-type eIF1, eIF1A, eIF3j, and eIF5 were prepared as described previously (8, 30). The concentrations of proteins, tRNA, and 40 S subunits were quantified by 280 or 260 nm absorbance.

Fluorescent Labeling of the Proteins—eIF1A-D142C and eIF3j-S152C single-cysteine mutants are used for modification with fluorescein as described previously, with minor modifications (30). Before the labeling reaction, 15 μl of protein (3 nmol) was reduced by adding 1 μl of 160 mM DTT and incubating for 2 h on ice. Note that all the following steps were carried out with degassed reagents and were kept in the dark as much as possible. The reduced protein was precipitated by adding 35 μl of saturated ammonium sulfate followed by a 10-min incubation at −20 °C. The precipitated protein was recovered by centrifugation at 20,000 × *g* for 30 min at 4 °C. The protein pellet was then washed briefly by adding 100 μl of 70% saturated ammonium sulfate and then pipetting it off to further remove residual DTT. The pellet was immediately dissolved in 50 μl of reaction buffer containing 20 mM potassium MES, pH 6.5, 0.3 M KCl, 1 mM EDTA, 10% glycerol, and 500 μM fluorescein-5-maleimide (Invitrogen). The reaction mixture was incubated in the dark for 2 h at room temperature and was quenched by adding 500 μl of buffer A (20 mM Hepes-K, pH 7.5, 2 mM DTT, and 10% glycerol). The labeled protein was captured by adding 40 μl of SP Sepharose resin (GE Healthcare). The resin was washed 4–6 times with 500 μl of buffer A containing 20 mM KCl until the absorbance at 492 nm reached a background level. The protein was eluted with 80 μl of buffer A containing 0.5 M KCl. Analysis by SDS-PAGE indicated that there was essentially no detectable free dye remaining in the eluate. The amounts of dye and the protein were quantified by 492 nm absorbance and Bradford assay using wild-type protein as a standard, typically yielding 1–2 nmol of the protein with ≥95% labeling efficiency. Fluorescent labeling of eIF1 was carried out by using the protein dual-labeling kit (Jena Bioscience) according to the manufacturer's protocol with minor modifications (33). The protein was expressed in BL21 (DE3) as a C-terminal fusion with the C-His_6-tagged intein and purified with 300 μl of nickel-nitrilotriacetic acid agarose resin. The intein was then cleaved by adding sodium 2-mercaptoethanesulfonate powder to a final concentration of ~0.5 M and incubating overnight in the dark at room temperature to produce a C-terminally thioesterified protein. The protein was purified with SP Sepharose resin as described above for eIF1A/eIF3j, but by using buffer A supplemented with 10 mM sodium 2-mercaptoethanesulfonate. The thioesterified protein was further oxyaminated by adding 2 μl of 1 M bisoxyamine to 6 μl of the protein eluate (~3 nmol) and incubating overnight at room temperature. To remove excess bisoxyamine, the protein was precipitated and washed with ammonium sulfate, as described above. The protein pellet (~2.5 nmol) was resuspended in 50 μl of reaction buffer containing 0.1 M sodium acetate, pH 5.6, 150 mM KCl, 10% glycerol, 100 mM aniline hydrochloride, and 1 mM keto-fluorescein. The reaction mixture was incubated for 2 h at room temperature and then overnight at 4 °C. The labeled protein was purified again with SP Sepharose resin, as described above. The labeling efficiency was typically ≥70%. The labeled proteins (termed eIF1-Fl, eIF1A-Fl, and eIF3j-Fl) were stored in a dark tube at −80 °C until use.

Translation Activity Assay—Translation assays were carried out in a messenger-dependent reticulocyte lysate system (Promega) essentially as described previously (34). The lysate was programed with a capped *Renilla* luciferase mRNA flanked by a human β-globin 5′-UTR. A 20-μl reaction mixture contained 50% nuclease-treated rabbit reticulocyte lysate, 20 μM amino

acid mixture minus leucine, 20 μM amino acid mixture minus methionine, 0.5 units/μl RNasin ribonuclease inhibitor, 45 mM potassium chloride, 90 mM potassium acetate, and 2 mM magnesium acetate. The mixture was preincubated with 1 μM WT-eIF, or 1 μM eIF-Fl for 5 min at 30 °C in the absence of mRNA. The reporter mRNA was then added to each reaction and further incubated at 30 °C for 30 min. Luminescence was measured for 10 s by using a VICTOR X5 plate reader (PerkinElmer) immediately after the addition of *Renilla* luciferase substrate (Promega). Luciferase activities were normalized to a reaction without adding the factors, and are presented as the average of three reactions ± S.D.

Fluorescence Anisotropy Binding Assay—Anisotropy measurements with eIF1-Fl, eIF1A-Fl, or eIF3j-Fl were conducted using a VICTOR X5 plate reader (PerkinElmer) with 485/15- and 535/25-nm emission and excitation filters with polarizers as described previously (30). The final concentration of the labeled species was limiting (5–20 nM), and the concentration of 40 S ribosomes was varied in each reaction. The concentrations of the additional factors were ≥90% saturating according to available affinities (this study): [eIF1] and [eIF1A] were 2 μM; [eIF5] was 4 μM; [eIF3j] was ≥2 μM depending on the affinity under the condition tested; [eIF3Δj] was 1 μM; and [eIF3] and [TC] were 650 nM or ≥[40 S] when [40 S] exceeded 650 nM. Increasing [eIF3] and [TC] 2-fold did not change the result, indicating that these components were well saturated at this concentration. The intact eIF3 was reconstituted by mixing stoichiometric amounts of eIF3j and eIF3Δj, and the TC was formed by mixing stoichiometric amounts of eIF2 and Met-tRNA$_i$ (typically 10 μM) in the presence of 100 μM GMPPNP and incubating for 3 min at 37 °C. Anisotropy binding reactions (20 μl for most reactions and 40 μl for reactions containing eIF1-Fl) were set up in binding buffer (20 mM Tris acetate, pH 7.5, 70 mM KCl, 2 mM $MgCl_2$, 10% glycerol, and 0.1 mg/ml BSA). When the TC was included in the reaction, 100 μM GMPPNP and 0.1 mg/ml creatine phosphokinase (to prevent nonspecific sticking of eIF2 (35)) were additionally included. Note that it is important to add eIF1-Fl to the reaction mixture at the very last step before incubation to minimize aggregation and/or sticking of eIF1 to the tube wall. This overcomes observing inconsistent fluorescent intensities from tube to tube. Importantly, the addition of BSA in the reaction buffer reduced nonspecific interactions and fluorescent quantum yield changes that otherwise often occur. This results in far more stable anisotropy readouts under the conditions tested. The reaction mixture was incubated for 3 min at 37 °C, and 18 or 36 μl was transferred to a 384-well plate and allowed to reach equilibrium at room temperature for 20 min before the anisotropy was measured. Anisotropy was converted to fraction of [eIF-Fl] bound and fitted to the solution of a quadratic equation describing an equilibrium reaction as described elsewhere (11). Inhibition constants (K_i) with an unlabeled wild-type protein were determined in a similar way to that described above, involving a preformed ribosomal complex of interest (containing a fluorescent-labeled protein) titrated with the corresponding unlabeled protein. Anisotropy was converted to fraction of [eIF-Fl] bound and fitted to the solution of a quadratic equation describing the competitive binding of two ligands to a receptor (36). All values reported are averages of at least three independent experiments, and the errors reported are standard deviations of the mean.

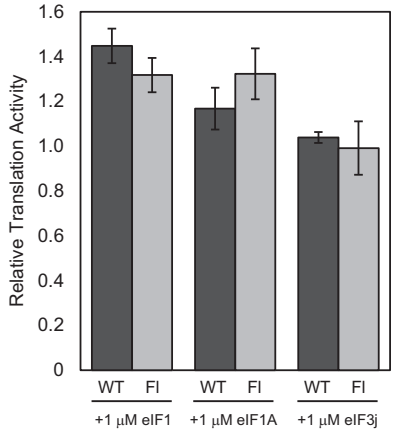

FIGURE 1. **Effect of fluorescent labeling on reticulocyte lysate translation.** 1 μM WT-eIF or eIF-Fl was added to a nuclease-treated lysate as indicated. Translation of a capped *Renilla* luciferase mRNA was quantified by measuring luminescence and was normalized to a reaction without adding the factor. The values shown are the mean of three independent experiments ± S.D.

RESULTS

Preparation and Characterization of Fluorescent-labeled eIF1, eIF1A, and eIF3j—To investigate the thermodynamic framework for human 43 S PIC formation, we first prepared fluorescent-labeled eIF1A and eIF3j (eIF1A-Fl and eIF3j-Fl) by modifying single-cysteine mutants with fluorescein, as described previously (30). A similar approach to modify human eIF1 was not successful because mutating the endogenous cysteines of eIF1 (Cys-69 and Cys-94) results in protein instability and a weakened binding to the 40 S subunit (data not shown (23)). Using an alternative approach, we prepared C-terminally thioesterified eIF1 and further modified it with bisoxyamine and keto-fluorescein (eIF1-Fl) (33). To determine whether modification of eIF1, eIF1A, and eIF3j preserves their function in the initiation pathway, we tested their activity by adding them to a reticulocyte lysate system. The addition of 1 μM of wild-type or modified protein to the lysate results in the same rate of translation (Fig. 1). Because this amount of protein is expected to be equimolar with the endogenous factor (37), we conclude that modification of each protein does not dramatically affect its activity. To examine the binding of each eIF to the 40 S subunit, purified 40 S subunits were titrated into a fixed amount of fluorescent-labeled eIF, and the change in fluorescence anisotropy was measured, as described under "Experimental Procedures." Individually, these fluorescent-labeled factors show a strong anisotropy increase upon 40 S titration (Table 1). Converting these values into the fraction of factor bound at each 40 S concentration yields equilibrium dissociation constants of 49, 62, and 8.8 nM for eIF1, eIF1A, and eIF3j, respectively (Fig. 2, *A–C*; also see Table 1 for K_d values). These values are in good agreement with previously determined K_d values for human eIF1A and eIF3j (19 and 6 nM (30)) and in reasonable agreement with those obtained for yeast eIF1 and eIF1A (16 and 49 nM (17)).

TABLE 1

Summary of K_d and anisotropy values

All values are the means of three independent experiments. The errors shown are the standard deviations. ND stands for not determined.

	K_d[a]	K_i[b]	r_{free}[c]	r_{bound}[d]	Δr_{max}[d]
eIF1-Fl					
40 S	49 ± 6	105 ± 9	0.264 ± 0.010	0.319 ± 0.012	0.055 ± 0.003
40 S + 1A	12 ± 0.4	39 ± 5	0.262 ± 0.013	0.336 ± 0.004	0.074 ± 0.009
40 S + 3j	72 ± 9	166 ± 8	0.258 ± 0.010	0.318 ± 0.003	0.060 ± 0.008
40 S + 1A + 3j	17 ± 5	41 ± 1	0.255 ± 0.006	0.331 ± 0.007	0.076 ± 0.012
40 S + 3	≤10	ND	0.289 ± 0.005	0.328 ± 0.008	0.039 ± 0.004
40 S + TC	27 ± 7	ND	0.266 ± 0.005	0.340 ± 0.008	0.075 ± 0.006
40 S + 1A + TC	≤10	ND	0.283 ± 0.003	0.348 ± 0.008	0.065 ± 0.007
40 S + 5	52 ± 5	ND	0.252 ± 0.006	0.308 ± 0.001	0.056 ± 0.005
43 S	≤10	ND	0.298 ± 0.005	0.375 ± 0.003	0.077 ± 0.003
eIF1A-Fl					
40 S	62 ± 5	61 ± 7	0.185 ± 0.002	0.240 ± 0.004	0.055 ± 0.001
40 S + 1	21 ± 2	23 ± 5	0.193 ± 0.003	0.250 ± 0.006	0.057 ± 0.003
40 S + 3j	230 ± 30	260 ± 60	0.190 ± 0.003	0.240 ± 0.002	0.050 ± 0.003
40 S + 1 + 3j	58 ± 3	53 ± 5	0.193 ± 0.005	0.244 ± 0.002	0.052 ± 0.006
40 S + 3	260 ± 30	ND	0.193 ± 0.003	0.245 ± 0.005	0.052 ± 0.007
40 S + 1 + 3	35 ± 3	ND	0.196 ± 0.008	0.237 ± 0.010	0.041 ± 0.003
40 S + TC	64 ± 5	ND	0.187 ± 0.006	0.221 ± 0.010	0.035 ± 0.006
40 S + 1 + TC	≤5	ND	0.212 ± 0.004	0.242 ± 0.003	0.030 ± 0.004
40 S + 5	55 ± 3	ND	0.194 ± 0.003	0.251 ± 0.003	0.056 ± 0.002
43 S	≤5	ND	0.205 ± 0.002	0.239 ± 0.002	0.033 ± 0.001
eIF3j-Fl					
40 S	8.8 ± 1.2	14 ± 2	0.193 ± 0.002	0.299 ± 0.003	0.106 ± 0.005
40 S + 1	18 ± 2	20 ± 3	0.179 ± 0.004	0.277 ± 0.003	0.098 ± 0.002
40 S + 1A	85 ± 9	110 ± 7	0.190 ± 0.004	0.292 ± 0.012	0.102 ± 0.009
40 S + 1 + 1A	~400[f]	~400[g]	0.182 ± 0.012	0.277 ± 0.019	0.095 ± 0.007
40 S + 3Δj	≤5	ND	0.234 ± 0.006	0.306 ± 0.003	0.072 ± 0.009
40 S + 1 + 3Δj	≤5	ND	0.217 ± 0.009	0.314 ± 0.009	0.097 ± 0.003
40 S + 1A + 3Δj	≤5	ND	0.215 ± 0.009	0.324 ± 0.003	0.109 ± 0.011
40 S + 1 + 1A + 3Δj	11 ± 2	ND	0.226 ± 0.007	0.296 ± 0.001	0.071 ± 0.006
40 S + TC	120 ± 20	ND	0.194 ± 0.004	0.314 ± 0.008	0.120 ± 0.011
40 S + 5	7.0 ± 1.2	ND	0.187 ± 0.003	0.273 ± 0.008	0.086 ± 0.006
43 S	15 ± 4	ND	0.216 ± 0.004	0.283 ± 0.001	0.067 ± 0.003
3Δj	100 ± 15	ND	0.171 ± 0.005	0.201 ± 0.005	0.030 ± 0.005

[a] Equilibrium dissociation constants determined by titrating the eIF-Fl with the 40 S subunit under the experimental condition.
[b] Equilibrium dissociation constants determined by titrating the unlabeled wild-type protein to the preformed eIF-Fl and 40 S complex under the experimental condition.
[c] Anisotropy of the indicated eIF-Fl prior to addition of 40 S subunits under the experimental conditions.
[d] Anisotropy of the indicated eIF-Fl in the 40 S bound state.
[e] Difference between r_{free} and r_{bound}, representing the maximum anisotropy change.
[f] The value was estimated from a titration ranging from [40 S] = 0 to 1100 nM.
[g] The value was calculated with using the estimate K_d value.

To further confirm that cysteine mutations and attachment of a fluorophore to these factors do not affect the interaction with the 40 S subunit, we titrated each preformed eIF-40 S complex with the corresponding non-labeled wild-type protein. Inhibition constants of 105, 61, and 14 nM were obtained for eIF1, eIF1A, and eIF3j, respectively, which are consistent with the equilibrium dissociation constants described above (Table 1). These data therefore established that these fluorescently modified proteins can be used to determine the thermodynamic framework of the 43 S PIC. It is important to note that we used a 5–20 nM concentration of each fluorescently labeled initiation factor to obtain a sufficient signal in our assay. Because this concentration was similar to some of the tight binding constants that we obtained, our measured K_ds were close to upper limits.

Human eIF1, eIF1A, and eIF3j Binding to the 40 S Ribosomes Is Thermodynamically Coupled—To explore whether eIF1, eIF1A, and eIF3j binding to the 40 S subunit is thermodynamically coupled, we employed our anisotropy assay with different combinations of these three factors. Initially, we measured the K_d for eIF1-Fl in the presence of a saturating amount of unlabeled eIF1A. A 4-fold decrease in the K_d of eIF1-Fl from 49 to 12 nM is observed upon the addition of unlabeled eIF1A (Fig. 2*A*), indicating a 4-fold increase in affinity. Likewise, we observe a 3-fold increase in the affinity of eIF1A-Fl upon the addition of unlabeled eIF1 (Fig. 2*B*). The results show that there is positive cooperativity between eIF1 and eIF1A.

We then performed similar experiments with eIF1A and eIF3j. Our data show that the affinity of eIF1A-Fl for the 40 S subunit decreases by 4-fold upon the addition of a saturating amount of eIF3j (Fig. 2*B*). Similarly, eIF3j-Fl binding to the 40 S subunit decreases in affinity by 10-fold upon the addition of a saturating eIF1A (Fig. 2*C*). The data show a strong negative cooperative effect on binding with eIF1A and eIF3j. In light of the positive cooperativity between eIF1 and eIF1A, we wanted to test whether the presence of eIF1 and eIF1A together would further weaken the affinity of eIF3j for the 40 S subunit. Our data show that this is indeed the case because the affinity of eIF3j-Fl binding to the 40 S subunit is further reduced by about 4-fold (K_d ~400 nM) in the presence of both eIF1 and eIF1A (Fig. 2*C*). It is important to note that this K_d only reflects an estimated value because it is not possible to obtain a saturated complex with eIF3j-Fl under these conditions. This is due to the fact that our anisotropy assay is limited by the concentration of 40 S subunits that can be added without causing anomalous anisotropy signals, possibly through aggregation and nonspecific binding. Consistent with the enhanced weakening of the interaction of eIF3j-Fl with the 40 S subunit in the presence of

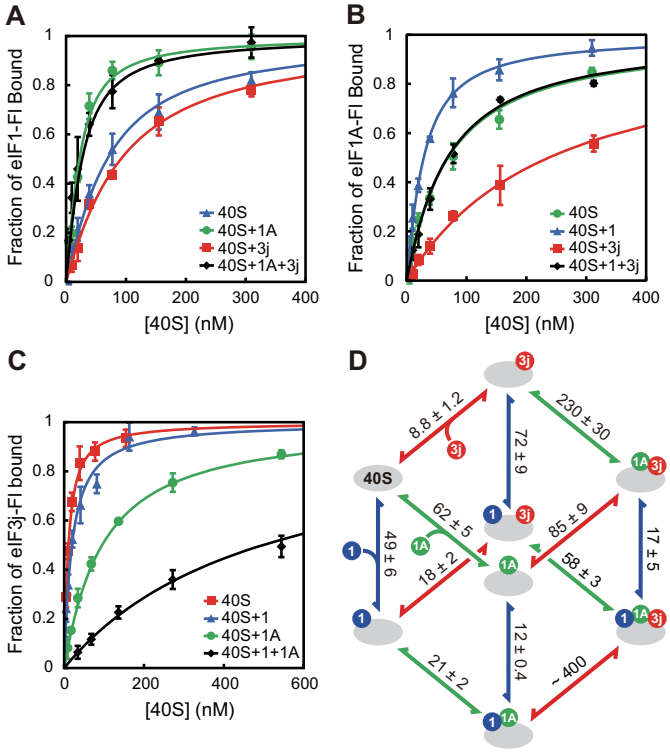

FIGURE 2. **Cooperativity between eIF1, eIF1A, and eIF3j for 40 S subunit binding.** *A*, equilibrium binding of eIF1-Fl to 40 S subunits in the absence or presence of saturating eIF1A and/or eIF3j, as measured by the anisotropy assay. Each point represents the mean of three independent experiments. *Error bars* indicate the S.D. *B*, equilibrium binding of eIF1A-Fl to the 40 S subunit in the absence or presence of saturating eIF1 and/or eIF3j. *Error bars* indicate the S.D. *C*, equilibrium binding of eIF3j-Fl to 40 S in the absence or presence of saturating of eIF1 and/or eIF1A. *D*, the thermodynamic framework for the binding of eIF1-Fl, eIF1A-Fl, and eIF3j-Fl to the 40 S subunit. *Blue*, *green*, *red*, and *gray circles* represent eIF1, eIF1A, and eIF3j and the 40 S subunit, respectively. Values alongside each *arrow* indicate K_d (in nM) for the corresponding binding.

both eIF1 and eIF1A, we find that the cooperative binding between eIF1 and eIF1A is maintained in the presence of eIF3j. This is indicated by a 4-fold increase in the affinity of eIF1A-Fl for the 40 S subunit in the presence of eIF3j when eIF1 is added (Fig. 2*B*). Likewise, the affinity of eIF1-Fl for the 40 S subunit in the presence of eIF3j increases by 4-fold when eIF1A is added (Fig. 2*A*). Finally, we explored whether eIF3j and eIF1 also may be thermodynamically coupled on the surface of the 40 S subunit. Our data show that the affinity of eIF3j-Fl binding to the 40 S subunit is in fact slightly reduced by 2-fold upon eIF1 binding (Fig. 2*C*). Accordingly, the affinity of eIF1-Fl binding to the 40 S subunit is also slightly reduced 1.5-fold in the presence of eIF3j (Fig. 2*A*), implying that eIF1 and eIF3j interact with each other on the surface of the 40 S subunit. Together, these data provide a complete thermodynamic framework of these three important initiation factors that bind to the decoding sites on the 40 S subunit (Fig. 2*D*), showing that all three are thermodynamically coupled on the surface of the 40 S subunit. It should be noted, however, that the decrease in the affinity of eIF3j-Fl for the 40 S subunit in the presence of eIF1A (either with or without eIF1) is possibly exaggerated because it is appreciably greater than the observed decrease of eIF1/eIF1A affinities in the corresponding condition.

Human eIF3 Stabilizes eIF1, eIF1A, and eIF3j Binding to the 40 S Subunit—Human eIF3j has been shown to promote the stable association of the eIF3 complex with the 40 S subunit by using sucrose gradient analysis (31, 38). Assuming that the binding of eIF3j and the rest of the eIF3 complex to the 40 S subunit is thermodynamically coupled, we wanted to test whether eIF3 can stabilize eIF3j binding to the 40 S subunit. Using an established protocol (30, 31), we purified eIF3 lacking the eIF3j subunit (eIF3Δj). We first determined the affinity of eIF3j to the eIF3Δj complex using our anisotropy assay. Titrating in eIF3Δj to eIF3j-Fl results in an appreciable change in anisotropy that is consistent with formation of the intact eIF3 complex. These data show that eIF3j binds to eIF3Δj with a reasonably strong affinity (K_d = 100 nM; Table 1). Importantly, eIF3j-Fl shows a lower anisotropy change when bound to eIF3Δj (0.030) as compared with that obtained upon 40 S binding (0.106; Table 1). This suggests that the site of fluorophore attachment in the C-terminal part of eIF3j is relatively flexible in the eIF3 complex and therefore allows us to detect 40 S binding in addition to eIF3 binding. Indeed, the anisotropy value of eIF3j is further increased by 0.072 when eIF3j-Fl in the eIF3 complex associates with the 40 S subunit (Table 1). The titration with the 40 S subunit indicates that the presence of the eIF3 complex increases eIF3j-Fl affinity about 2-fold ($K_d \leq 5$ nM as compared with 8.8 nM; Table 1). Because the concentration of eIF3j-Fl in our assay is 5 nM, the K_d of eIF3j-Fl binding to the 40 S subunit in the presence of eIF3Δj is therefore an upper limit.

In light of our data indicating that eIF1 and eIF1A weaken the affinity of eIF3j for the 40 S subunit, we tested whether eIF3Δj stabilizes eIF3j in the presence of these factors. Using our anisotropy assay, we show that the stabilizing effect of eIF3Δj on eIF3j-Fl binding is much more evident when a saturating concentration of eIF1A or both eIF1 and eIF1A are present. In these complexes, the affinity of eIF3j for the 40 S subunit is at least 20-fold increased as compared with the complexes without eIF3Δj (Fig. 3*C*; also see Table 1 for K_d values). Taken together, these data indicate that the whole eIF3 complex plays a key role in stabilizing eIF3j in the 40 S subunit decoding site in the presence of eIF1 and eIF1A.

It had been shown previously that eIF1 interacts with eIF3c in yeast and mammals (20, 39, 40). To test whether human eIF3 and eIF1 are thermodynamically coupled on the 40 S subunit, we determined the affinity of eIF1-Fl for the 40 S subunit in the presence of eIF3. In the absence of the 40 S subunit, the addition of eIF3 to eIF1-Fl slightly increases the anisotropy value by 0.025 (Table 1), consistent with an interaction between eIF1-Fl and eIF3. The addition of the 40 S subunit further increases the anisotropy by 0.039, allowing us to detect a 40 S-specific anisotropy change. Upon the addition of eIF3, the affinity of eIF1-Fl is increased by over 7-fold (Fig. 3*A*). This indicates that the whole eIF3 complex also plays a role in stabilizing eIF1 binding to the 40 S subunit.

It has been shown that eIF3 can interact with eIF1A in the absence and presence of the 40 S subunit (6, 41, 42). We therefore used our anisotropy assay to investigate whether we can observe thermodynamic coupling between eIF3 and eIF1A on the surface of the 40 S subunit. The complete eIF3 complex

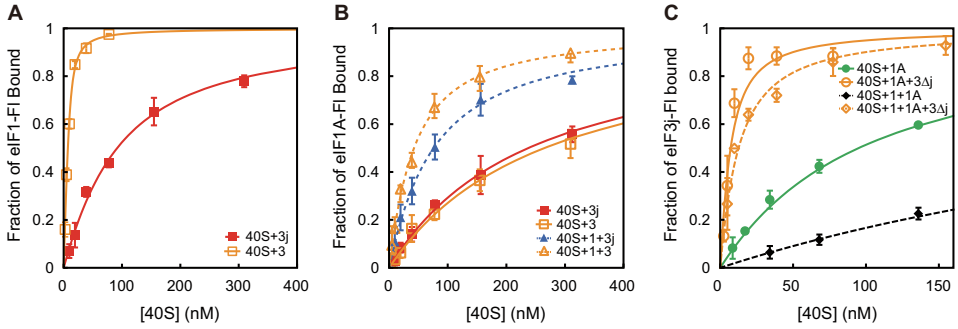

FIGURE 3. **Effect of the eIF3 complex on eIF1, eIF1A, or eIF3j binding to the 40 S subunit.** *A*, equilibrium binding of eIF1-Fl to the 40 S subunit in the presence of saturating eIF3j or eIF3, as in Fig. 1*A*. *B*, equilibrium binding of eIF1A-Fl to 40 S and to 40 S+eIF1 in the presence of saturating eIF3j or eIF3. *C*, equilibrium binding of eIF3j-Fl to 40 S+eIF1A and to 40 S+eIF1+eIF1A in the absence or presence of saturating eIF3Δj. Each point represents the mean of three independent experiments. *Error bars* indicate the S.D.

shows the same degree of negative cooperativity with eIF1A as compared with eIF3j (Fig. 3*B*). Interestingly, this negative cooperativity becomes slightly less apparent in the presence of eIF1 (1.5-fold decrease in the affinity of eIF1A-Fl as compared with a 3-fold decrease caused by eIF3j alone). This indicates that the whole eIF3 complex does help to indirectly stabilize eIF1A binding to the 40 S subunit, albeit to a small degree.

The eIF2 Ternary Complex Stabilizes eIF1 and eIF1A on the 40 S Subunit—It has been well demonstrated that eIF1 and eIF1A cooperatively promote recruitment of the eIF2-GTP-Met-tRNA$_i$ TC to the 40 S subunit in yeast and mammals (6, 9, 14, 41, 43). Our previous work has shown that eIF1 is able to stably bind to eIF2 using a gel-shift assay (8). Interestingly, we are not able to detect this interaction using our anisotropy assay (compare r_{free} values with or without the TC in Table 1). Although this may imply that eIF1-Fl does not interact directly with the TC under the conditions used, it may also indicate that the interaction between eIF1-Fl and TC does not cause a detectable anisotropy change. We verified that eIF1-Fl does form a stable complex with the TC using our native gel electrophoresis assay (data not shown). The affinity of eIF1-Fl for the 40 S subunit is increased roughly 2-fold upon the addition of TC (Fig. 4*A*; also see Table 1 for K_d values). This is consistent with a direct or indirect interaction between eIF1 and TC on the surface of the 40 S subunit. A similar level of affinity increase by the TC is observed when saturating eIF1A is present (Fig. 4*A*), indicating that both eIF1A and the TC can stabilize eIF1 binding at the same time. This is consistent with a previous sucrose gradient analysis showing that eIF1 binds tighter to the 40 S subunit when eIF1A and TC are present (6).

We also used our anisotropy assay to investigate whether TC changes the affinity of eIF1A-Fl for the 40 S. Surprisingly, we find that the affinity of eIF1A for the 40 S subunit is not altered upon TC binding (Fig. 4*B*). In contrast, upon the addition of eIF1, the TC increases the affinity of eIF1A-Fl for the 40 S subunit by at least 4-fold. Interestingly, in all conditions tested in the presence of TC, the average anisotropy change (Δr_{max}) of eIF1A-Fl is consistently decreased to ~0.03 as compared with that in the absence of the TC (~0.05; Table 1), possibly indicating that the conformation of the eIF1A C-terminal tail (where the fluorophore is attached) becomes more flexible in the presence of the TC.

Because eIF3j has not been shown to interact with the TC, we used our assay to determine whether the TC can also affect the stability of eIF3j on the ribosome. In the absence of other initiation factors, the presence of the TC strongly destabilizes eIF3j binding by decreasing the affinity of eIF3j-Fl for the 40 S subunit by over 10-fold (Fig. 4*C*). It is possible that the previously identified conformational change in the 40 S subunit upon TC binding may be responsible for the change in eIF3j-Fl affinity (44).

eIF1, eIF1A, and eIF3j Stably Bind to the 43 S Preinitiation Complex—Because we have addressed both negative and positive effects of eIF3 and TC on the thermodynamics of the tested factors, we wanted to determine the 40 S binding stabilities of these factors in the presence of both eIF3 and TC. To this end, we tested individual factor binding to 40 S complexes comprising eIF1, eIF1A, eIF3 and the TC. We eliminated eIF5 in the following assays for simplicity because eIF1, eIF1A, and eIF3j binding to the 40 S subunit individually is not changed in the presence of eIF5 (Table 1). Our data reveal that the K_d of eIF1A-Fl binding to the 43 S PIC is ≤5 nM (Fig. 4*B*). This value is lower than the K_d of 35 nM in the absence of the TC, but the same as the K_d in the absence of eIF3, indicating that eIF1A tightly associates with the 43 S PIC through stabilizing effects by eIF1 and the TC (mediated by eIF1). Our data also reveal that eIF3j binds to the 43 S PIC with a K_d of 17 nM (Fig. 4*C*), which is far lower than the value obtained without eIF3Δj (~400 nM). This indicates that the whole eIF3 complex is critical for high affinity eIF3j binding on the 43 S PIC. As expected, eIF1-Fl binding to the 43 S PIC is very tight (K_d ≤10 nM) and is immediately saturated at ~20 nM [40 S] (Fig. 4*A*). This is likely to reflect that all the other components of the 43 S PIC, with the exception of eIF3j, have been shown to significantly stabilize eIF1 binding to the 40 S subunit.

DISCUSSION

In this study, we have conducted a quantitative analysis of human 43 S PIC formation using fluorescently labeled eIF1, eIF1A, and eIF3j as molecular probes. By testing the affinity of these components in a number of different 40 S subunit complexes, we have discovered that a complicated network of interactions is required to stabilize the 43 S PIC. A summary of the negative and positive cooperativity observed between the 43 S PIC components and the 40 S subunit is shown in Fig. 5. Impor-

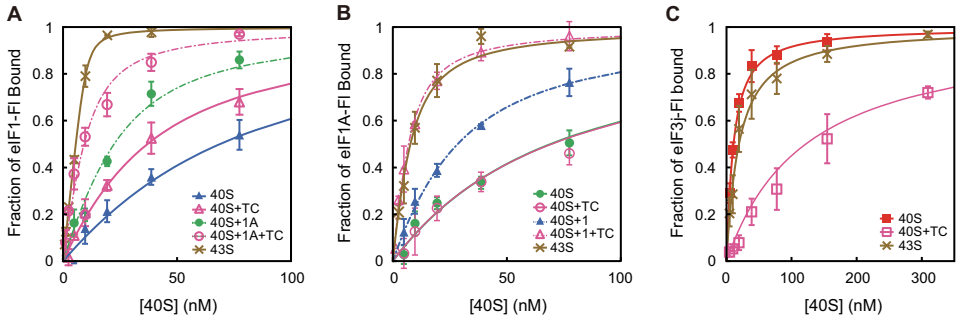

FIGURE 4. **Effect of TC on eIF1, eIF1A, or eIF3j binding to the 40 S subunit.** *A*, equilibrium binding of eIF1-FI to 40 S/40 S+eIF1A in the absence or presence of saturating TC, or to the 43 S PIC, as in Fig. 1*A*. *B*, equilibrium binding of eIF1A-FI to 40 S/40 S+eIF1 in the absence or presence of saturating TC, or to the 43 S PIC. *C*, equilibrium binding of eIF3j-FI to 40 S in the absence or presence of saturating TC, or to the 43 S PIC. Each point represents the mean of three independent experiments. *Error bars* indicate the S.D.

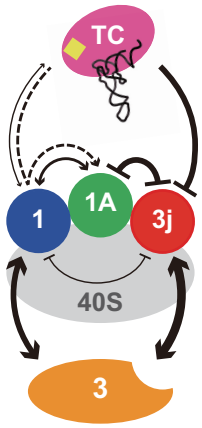

FIGURE 5. **Cooperativity among factors within the 43 S PIC.** Positive and negative cooperativity are indicated as *arrows* and *bar-headed lines*, respectively. *Dashed arrows* indicate indirect stabilization mediated by eIF1. The thickness of the lines represents relative strength of the effect.

tantly, our data reveal central roles of eIF3 and the TC in stabilizing eIF1, eIF1A, and eIF3j on the 40 S subunit.

Here, we show that eIF1 and eIF1A bind cooperatively to the 40 S subunit with an ~4-fold thermodynamic coupling. This is in good agreement with the 4–8-fold coupling between these factors in the yeast system, indicating that this interaction is conserved through evolution (13, 17, 18). Although it has not been tested in the yeast system, we now reveal that eIF3j and eIF3 also bind cooperatively with the 40 S. This explains the finding that eIF3j stabilizes the eIF3 complex on the 40 S subunit during sucrose gradient centrifugation in yeast and humans (30, 45). Because eIF3j easily dissociates from the eIF3 complex during purification (30–32), it is often assumed that this protein is not an integral part of eIF3 or the 43 S PIC. By revealing the cooperative binding of eIF3j and eIF3 to the 43 S PIC, our data now show that eIF3j is in fact as tightly associated with this complex as eIF1 and eIF1A. Moreover, the affinity that we measure here suggests that the 43 S PIC is likely saturated with eIF3j under physiological concentrations (see below). This highlights the importance of thermodynamic measurements for obtaining an accurate representation of the interactions between components of complex systems such as the 43 S PIC.

Our data demonstrate different degrees of negative cooperativity between eIF3j and the binding of eIF1, eIF1A, and TC to the 40 S subunit (Fig. 5). Previous work has shown that the C-terminal half of human eIF3j binds to the mRNA entry channel and A-site of the 40 S subunit, enabling it to dramatically lower the affinity of mRNA for the 40 S subunit decoding site (30, 44). In the absence of eIF3, the binding of eIF1, eIF1A, and TC reverses the inhibitory activity of eIF3j on mRNA binding to the 40 S subunit (30). Our quantitative data now provide an explanation for this result because the binding of eIF1, eIF1A, and the TC appreciably lowers eIF3j affinity to the 40 S subunit. In the presence of eIF3, human eIF3j is released from the mRNA entry channel and A-site upon TC binding and a conformational change induced by domain II of the hepatitis C virus internal ribosome entry site (44). Interestingly, a site-directed cleavage assay indicates that domain II of the hepatitis C virus internal ribosome entry site induces a similar conformational change in the 40 S as found for eIF1 and eIF1A binding (44). Therefore, it is likely that eIF1, eIF1A, and the TC will all play an important role in releasing eIF3j from the decoding site of the 40 S subunit upon mRNA recruitment. Nevertheless, a detailed kinetic analysis of capped mRNA recruitment and the role of canonical initiation factors on eIF3j displacement from the decoding site will be required to fully understand this complicated process. It is interesting to note that the release of eIF3j from the mRNA entry channel would likely result in a stabilizing effect on eIF1, eIF1A, and TC binding to the 40 S subunit. Such an increase in eIF1, eIF1A, and TC affinity for the 40 S subunit upon eIF3j dissociation may be important in stabilizing mRNA in the decoding site of the 40 S subunit. It is noteworthy to mention that although eIF3j dissociates from the mRNA entry channel and A-site of the 40 S subunit upon mRNA recruitment, its interaction with eIF3 likely prevents it from completely dissociating from the scanning 40 S subunit. This would be consistent with the finding that eIF3j increases the fidelity of initiation codon selection in yeast through a direct or indirect interaction with eIF1A (46). A quantitative study of the interaction between eIF3j and the 43 S PIC has not yet been carried out in the yeast system, but we expect that the interactions that we have revealed here will be conserved through evolution.

The eIF3 complex has been shown to stabilize eIF1, eIF1A, and TC on the surface of the 40 S subunit using non-equilibrium assays (6–8). However, the interaction between eIF3 and the initiation factors in the 43 S PIC has not been investigated using equilibrium binding assays. Our data now reveal that eIF3 is thermodynamically coupled with eIF1, eIF1A, and eIF3j in

the 43 S PIC. Specifically, the human eIF3 complex increases the affinity of eIF1 for the 40 S subunit at least 5-fold (to the limit of detection). In addition, eIF3 increases the affinity of eIF1A for the 40 S subunit by 7-fold, but only in the presence of eIF1. The thermodynamic coupling between eIF3 and eIF1 agrees well with the direct interaction between these factors in the multifactor complex (20, 47). In the absence of eIF3, eIF1 dissociates from the 43 S PIC upon initiation codon selection in yeast (9, 12). In light of our data showing a strong thermodynamic coupling between eIF3 and eIF1, it will now be important to determine whether eIF3 has any impact on the release of eIF1 upon start codon selection.

Our data reveal an important role of the TC in increasing the affinity of eIF1 and eIF1A on the 40 S subunit. We show that the affinity of eIF1A is increased by 3-fold in the presence of eIF1 and by a further 5-fold upon the addition of TC (Table 1). Our data are in good agreement with that shown previously for the yeast system, where eIF1, eIF1A, and TC are thermodynamically coupled in the absence of mRNA. Specifically, the affinity of yeast eIF1A is increased 4-fold by the addition of eIF1 and a further 30-fold when TC is added (13). It should be noted that upon the addition of TC to this complex in our assay, the affinity of eIF1A for the 40 S subunit is at the level of detection due to the concentration of eIF1A used. Therefore, the total increase in affinity of eIF1A in the presence of eIF1 and TC in our assay may be an underestimation. Interestingly, we show that TC can only increase the affinity of eIF1A binding to the 40 S subunit in the presence of eIF1. Therefore, the positive cooperativity between eIF1 and eIF1A appears to play an important role in transmitting the stabilizing effect of TC on eIF1A in the absence of mRNA. Although the coupling between eIF1 and eIF1A is necessary for stabilizing TC binding in the absence of mRNA (Table 1) (13), it is interesting to note that eIF1A is able to accelerate binding and increase the affinity of the TC independently of eIF1 in the presence of an AUG-containing mRNA (19). This likely indicates that there is an appreciable rearrangement in the interactions between eIF1, eIF1A, and the TC upon mRNA recruitment and start codon recognition.

Previous work has shown that yeast and human eIF5 interacts with eIF1, eIF3, and TC in the absence of the 40 S subunit (8, 20). It is also clear that eIF5 plays an important role in initiation codon selection, most likely through changes in direct and indirect interactions with eIF1, eIF1A, and eIF2 on the surface of the 40 S subunit (11, 15, 48). Although we have not determined whether there is a contribution of eIF5 on the overall stability of the 43 S PIC, we do not observe any influence of eIF5 on the stability of eIF1, eIF1A, or eIF3j individually with the 40 S subunit (Table 1). Nevertheless, we cannot rule out a possible influence of eIF5 on the stability of these components in the presence of eIF3 and TC, although the stability of this complex is already close to our detection limit (5–10 nM). An alternative approach will therefore likely be needed to determine how eIF5 influences the stability of the 43 S PIC in the human system. It is worth noting that the overexpression of human eIF5 decreases the stringency of start codon selection (49), suggesting that eIF5 is not required for initial mRNA recruitment to the 43 S PIC.

What is the biological significance of the affinity changes observed here? In certain conditions, they could play an important role in promoting factor binding to the 40 S subunit. For example, eIF1A binding is substantially destabilized by eIF3 to a K_d of 260 nM, but is ~7-fold stabilized by the addition of eIF1. Assuming the physiological concentrations of mammalian initiation factors and ribosomes are roughly at least 1000 nM (50), eIF1A would therefore be subsaturating without the positive cooperativity of eIF1 binding to the 40 S subunit. However, in the presence of other PIC components, the affinities are considerably tighter regardless of the observed positive or negative cooperativity ($K_d < 100$ nM). Thus, we would expect that these individual factors are likely to be saturated on the surface of the 40 S subunit under physiological concentrations. Consistent with this, it is suggested in yeast cells that the rate of translation is relatively insensitive to the cellular concentration of most initiation factors (51), implying that they are indeed saturating. Therefore, the changes in affinity that we observe may have no obvious effect on the saturation of complexes *per se*, with the possible exception of eIF3j. Instead, it is possible that the changes in affinity signify conformational changes in the 40 S subunit decoding site that are important in subsequent mRNA binding and scanning steps. Consistent with this, conformational rearrangements of the 40 S mRNA entry channel and decoding site have been observed using a site-directed hydroxyl radical cleavage assay to monitor eIF1, eIF1A, eIF3, and TC recruitment (44). In addition, one can also speculate that an observed increase in affinity may be important in prolonging the lifetime of individual initiation factors on the 40 S subunit during the initiation pathway. Any change in lifetime of these initiation factors could dramatically change the availability of the 43 S PIC for entering the initiation pathway.

The thermodynamic framework that we present here provides a more complete quantitative understanding of the interactions between components of the human 43 S PIC. This framework helps to explain the importance of eIF3 and TC on maintaining the affinity of eIF1, eIF1A, and eIF3j on the surface of the 40 S subunit (Fig. 5). It will now be important to quantitatively determine the association and dissociation rates of these initiation components on the 40 S subunit during different stages of initiation. The importance of knowing the lifetimes of each component bound to the 43 S PIC is particularly well illustrated by the elucidation of the kinetics of eIF1 release from the 40 S subunit during initiation codon recognition (9, 12, 15). Our data now indicate that a mechanism to release eIF3j from the mRNA entry channel must also exist, but it is not yet clear what specific PIC components accelerate its dissociation upon mRNA recruitment.

Acknowledgments—We thank John Hershey and the Fraser laboratory for many insightful comments and critical reading of the manuscript.

REFERENCES

1. Mathews, M. B., Sonenberg, N., and Hershey, J. W. B. (2007) *Translational Control in Biology and Medicine* (Mathews, M. B., Sonenberg, N., and Hershey, J. W. B., eds), pp. 87–128, Cold Spring Harbor Laboratory Press, Cold Spring Harbor, NY

2. Lorsch, J. R., and Dever, T. E. (2010) Molecular view of 43 S complex formation and start site selection in eukaryotic translation initiation. *J. Biol. Chem.* **285,** 21203–21207
3. Hinnebusch, A. G. (2014) The scanning mechanism of eukaryotic translation initiation. *Annu. Rev. Biochem.* **83,** 779–812
4. Thomas, A., Goumans, H., Voorma, H. O., and Benne, R. (1980) The mechanism of action of eukaryotic initiation factor 4C in protein synthesis. *Eur. J. Biochem.* **107,** 39–45
5. Chaudhuri, J., Si, K., and Maitra, U. (1997) Function of Eukaryotic translation initiation factor 1A (eIF1A) (formerly called eIF-4C) in initiation of protein synthesis. *J. Biol. Chem.* **272,** 7883–7891
6. Majumdar, R., Bandyopadhyay, A., and Maitra, U. (2003) Mammalian translation initiation factor eIF1 functions with eIF1A and eIF3 in the formation of a stable 40 S preinitiation complex. *J. Biol. Chem.* **278,** 6580–6587
7. Algire, M. A., Maag, D., Savio, P., Acker, M. G., Tarun, S. Z., Jr., Sachs, A. B., Asano, K., Nielsen, K. H., Olsen, D. S., Phan, L., Hinnebusch, A. G., and Lorsch, J. R. (2002) Development and characterization of a reconstituted yeast translation initiation system. *RNA* **8,** 382–397
8. Sokabe, M., Fraser, C. S., and Hershey, J. W. B. (2012) The human translation initiation multi-factor complex promotes methionyl-tRNA$_i$ binding to the 40S ribosomal subunit. *Nucleic Acids Res.* **40,** 905–913
9. Maag, D., Fekete, C. A., Gryczynski, Z., and Lorsch, J. R. (2005) A conformational change in the eukaryotic translation preinitiation complex and release of eIF1 signal recognition of the start codon. *Mol. Cell* **17,** 265–275
10. Fekete, C. A., Applefield, D. J., Blakely, S. A., Shirokikh, N., Pestova, T., Lorsch, J. R., and Hinnebusch, A. G. (2005) The eIF1A C-terminal domain promotes initiation complex assembly, scanning and AUG selection *in vivo*. *EMBO J.* **24,** 3588–3601
11. Maag, D., Algire, M. A., and Lorsch, J. R. (2006) Communication between eukaryotic translation initiation factors 5 and 1A within the ribosomal pre-initiation complex plays a role in start site selection. *J. Mol. Biol.* **356,** 724–737
12. Cheung, Y.-N., Maag, D., Mitchell, S. F., Fekete, C. A., Algire, M. A., Takacs, J. E., Shirokikh, N., Pestova, T., Lorsch, J. R., and Hinnebusch, A. G. (2007) Dissociation of eIF1 from the 40S ribosomal subunit is a key step in start codon selection *in vivo*. *Genes Dev.* **21,** 1217–1230
13. Fekete, C. A., Mitchell, S. F., Cherkasova, V. A., Applefield, D., Algire, M. A., Maag, D., Saini, A. K., Lorsch, J. R., and Hinnebusch, A. G. (2007) N- and C-terminal residues of eIF1A have opposing effects on the fidelity of start codon selection. *EMBO J.* **26,** 1602–1614
14. Saini, A. K., Nanda, J. S., Lorsch, J. R., and Hinnebusch, A. G. (2010) Regulatory elements in eIF1A control the fidelity of start codon selection by modulating tRNA$_i^{Met}$ binding to the ribosome. *Genes Dev.* **24,** 97–110
15. Nanda, J. S., Saini, A. K., Muñoz, A. M., Hinnebusch, A. G., and Lorsch, J. R. (2013) Coordinated movements of eukaryotic translation initiation factors eIF1, eIF1A, and eIF5 trigger phosphate release from eIF2 in response to start codon recognition by the ribosomal preinitiation complex. *J. Biol. Chem.* **288,** 5316–5329
16. Dong, J., Munoz, A., Kolitz, S. E., Saini, A. K., Chiu, W. L., Rahman, H., Lorsch, J. R., and Hinnebusch, A. G. (2014) Conserved residues in yeast initiator tRNA calibrate initiation accuracy by regulating preinitiation complex stability at the start codon. *Genes Dev.* **28,** 502–520
17. Maag, D., and Lorsch, J. R. (2003) Communication between eukaryotic translation initiation factors 1 and 1A on the yeast small ribosomal subunit. *J. Mol. Biol.* **330,** 917–924
18. Nanda, J. S., Cheung, Y.-N., Takacs, J. E., Martin-Marcos, P., Saini, A. K., Hinnebusch, A. G., and Lorsch, J. R. (2009) eIF1 controls multiple steps in start codon recognition during eukaryotic translation initiation. *J. Mol. Biol.* **394,** 268–285
19. Passmore, L. A., Schmeing, T. M., Maag, D., Applefield, D. J., Acker, M. G., Algire, M. A., Lorsch, J. R., and Ramakrishnan, V. (2007) The eukaryotic translation initiation factors eIF1 and eIF1A induce an open conformation of the 40S ribosome. *Mol. Cell* **26,** 41–50
20. Asano, K., Clayton, J., Shalev, A., and Hinnebusch, A. G. (2000) A multifactor complex of eukaryotic initiation factors, eIF1, eIF2, eIF3, eIF5, and initiator tRNA^{Met} is an important translation initiation intermediate *in vivo*. *Genes Dev.* **14,** 2534–2546
21. Dennis, M. D., Person, M. D., and Browning, K. S. (2009) Phosphorylation of plant translation initiation factors by CK2 enhances the *in vitro* interaction of multifactor complex components. *J. Biol. Chem.* **284,** 20615–20628
22. Hinnebusch, A. G., and Lorsch, J. R. (2012) The mechanism of eukaryotic translation initiation: new insights and challenges. *Cold Spring Harb. Perspect. Biol.* **4,** a011544
23. Lomakin, I. B., Kolupaeva, V. G., Marintchev, A., Wagner, G., and Pestova, T. V (2003) Position of eukaryotic initiation factor eIF1 on the 40S ribosomal subunit determined by directed hydroxyl radical probing. *Genes Dev.* **17,** 2786–2797
24. Rabl, J., Leibundgut, M., Ataide, S. F., Haag, A., and Ban, N. (2011) Crystal structure of the eukaryotic 40S ribosomal subunit in complex with initiation factor 1. *Science* **331,** 730–736
25. Yu, Y., Marintchev, A., Kolupaeva, V. G., Unbehaun, A., Veryasova, T., Lai, S.-C., Hong, P., Wagner, G., Hellen, C. U. T., and Pestova, T. V (2009) Position of eukaryotic translation initiation factor eIF1A on the 40S ribosomal subunit mapped by directed hydroxyl radical probing. *Nucleic Acids Res.* **37,** 5167–5182
26. Weisser, M., Voigts-Hoffmann, F., Rabl, J., Leibundgut, M., and Ban, N. (2013) The crystal structure of the eukaryotic 40S ribosomal subunit in complex with eIF1 and eIF1A. *Nat. Struct. Mol. Biol.* **20,** 1015–1017
27. Lomakin, I. B., and Steitz, T. A. (2013) The initiation of mammalian protein synthesis and mRNA scanning mechanism. *Nature* **500,** 307–311
28. Pisarev, A. V., Kolupaeva, V. G., Pisareva, V. P., Merrick, W. C., Hellen, C. U. T., and Pestova, T. V (2006) Specific functional interactions of nucleotides at key −3 and +4 positions flanking the initiation codon with components of the mammalian 48S translation initiation complex. *Genes Dev.* **20,** 624–636
29. Shin, B.-S., Kim, J.-R., Walker, S. E., Dong, J., Lorsch, J. R., and Dever, T. E. (2011) Initiation factor eIF2γ promotes eIF2-GTP-Met-tRNA$_i^{Met}$ ternary complex binding to the 40S ribosome. *Nat. Struct. Mol. Biol.* **18,** 1227–1234
30. Fraser, C. S., Berry, K. E., Hershey, J. W. B., and Doudna, J. A. (2007) eIF3j is located in the decoding center of the human 40S ribosomal subunit. *Mol. Cell* **26,** 811–819
31. Fraser, C. S., Lee, J. Y., Mayeur, G. L., Bushell, M., Doudna, J. A., and Hershey, J. W. B. (2004) The j-subunit of human translation initiation factor eIF3 is required for the stable binding of eIF3 and its subcomplexes to 40 S ribosomal subunits *in vitro*. *J. Biol. Chem.* **279,** 8946–8956
32. Valásek, L., Phan, L., Schoenfeld, L. W., Valásková, V., and Hinnebusch, A. G. (2001) Related eIF3 subunits TIF32 and HCR1 interact with an RNA recognition motif in PRT1 required for eIF3 integrity and ribosome binding. *EMBO J.* **20,** 891–904
33. Yi, L., Sun, H., Wu, Y.-W., Triola, G., Waldmann, H., and Goody, R. S. (2010) A highly efficient strategy for modification of proteins at the C terminus. *Angew. Chem. Int. Ed. Engl.* **49,** 9417–9421
34. Feoktistova, K., Tuvshintogs, E., Do, A., and Fraser, C. S. (2013) Human eIF4E promotes mRNA restructuring by stimulating eIF4A helicase activity. *Proc. Natl. Acad. Sci. U.S.A.* **110,** 13339–13344
35. Benne, R., Amesz, H., Hershey, J. W. B., and Voorma, H. O. (1979) The activity of eukaryotic initiation factor eIF-2 in ternary complex formation with GTP and Met-tRNA$_f$. *J. Biol. Chem.* **254,** 3201–3205
36. Weeks, K. M., and Crothers, D. M. (1992) RNA binding assays for Tat-derived peptides: implications for specificity. *Biochemistry* **31,** 10281–10287
37. Barth-Baus, D., Bhasker, C., Zoll, W., and Merrick, W. C. (2013) Influence of translation factor activities on start site selection in six different mRNAs. *Translation* **1,** 10.4161/trla.24419
38. Unbehaun, A., Borukhov, S. I., Hellen, C. U. T., and Pestova, T. V (2004) Release of initiation factors from 48S complexes during ribosomal subunit joining and the link between establishment of codon-anticodon base-pairing and hydrolysis of eIF2-bound GTP. *Genes Dev.* **18,** 3078–3093
39. Fletcher, C. M., Pestova, T. V., Hellen, C. U. T., and Wagner, G. (1999) Structure and interactions of the translation initiation factor eIF1. *EMBO J.* **18,** 2631–2637
40. Phan, L., Schoenfeld, L. W., Valásek, L., Nielsen, K. H., and Hinnebusch, A. G. (2001) A subcomplex of three eIF3 subunits binds eIF1 and eIF5 and

stimulates ribosome binding of mRNA and $tRNA_i^{Met}$. *EMBO J.* **20,** 2954–2965
41. Olsen, D. S., Savner, E. M., Mathew, A., Zhang, F., Krishnamoorthy, T., Phan, L., and Hinnebusch, A. G. (2003) Domains of eIF1A that mediate binding to eIF2, eIF3 and eIF5B and promote ternary complex recruitment *in vivo*. *EMBO J.* **22,** 193–204
42. Sun, C., Todorovic, A., Querol-Audí, J., Bai, Y., Villa, N., Snyder, M., Ashchyan, J., Lewis, C. S., Hartland, A., Gradia, S., Fraser, C. S., Doudna, J. A., Nogales, E., and Cate, J. H. D. (2011) Functional reconstitution of human eukaryotic translation initiation factor 3 (eIF3). *Proc. Natl. Acad. Sci. U.S.A.* **108,** 20473–20478
43. Martin-Marcos, P., Nanda, J., Luna, R. E., Wagner, G., Lorsch, J. R., and Hinnebusch, A. G. (2013) β-Hairpin loop of eukaryotic initiation factor 1 (eIF1) mediates 40 S ribosome binding to regulate initiator $tRNA^{Met}$ recruitment and accuracy of AUG selection *in vivo*. *J. Biol. Chem.* **288,** 27546–27562
44. Fraser, C. S., Hershey, J. W. B., and Doudna, J. A. (2009) The pathway of hepatitis C virus mRNA recruitment to the human ribosome. *Nat. Struct. Mol. Biol.* **16,** 397–404
45. Nielsen, K. H., Valásek, L., Sykes, C., Jivotovskaya, A., and Hinnebusch, A. G. (2006) Interaction of the RNP1 motif in PRT1 with HCR1 promotes 40S binding of eukaryotic initiation factor 3 in yeast. *Mol. Cell Biol.* **26,** 2984–2998
46. Elantak, L., Wagner, S., Herrmannová, A., Karásková, M., Rutkai, E., Lukavsky, P. J., and Valásek, L. (2010) The indispensable N-terminal half of eIF3j/HCR1 cooperates with its structurally conserved binding partner eIF3b/PRT1-RRM and with eIF1A in stringent AUG selection. *J. Mol. Biol.* **396,** 1097–1116
47. Reibarkh, M., Yamamoto, Y., Singh, C. R., del Rio, F., Fahmy, A., Lee, B., Luna, R. E., Ii, M., Wagner, G., and Asano, K. (2008) Eukaryotic initiation factor (eIF) 1 carries two distinct eIF5-binding faces important for multifactor assembly and AUG selection. *J. Biol. Chem.* **283,** 1094–1103
48. Martin-Marcos, P., Nanda, J. S., Luna, R. E., Zhang, F., Saini, A. K., Cherkasova, V. A., Wagner, G., Lorsch, J. R., and Hinnebusch, A. G. (2014) Enhanced eIF1 binding to the 40S ribosome impedes conformational rearrangements of the preinitiation complex and elevates initiation accuracy. *RNA* **20,** 150–167
49. Loughran, G., Sachs, M. S., Atkins, J. F., and Ivanov, I. P. (2012) Stringency of start codon selection modulates autoregulation of translation initiation factor eIF5. *Nucleic Acids Res.* **40,** 2898–2906
50. Duncan, R., and Hershey, J. W. B. (1983) Identification and quantitation of levels of protein synthesis initiation factors in crude HeLa cell lysates by two-dimensional polyacrylamide gel electrophoresis. *J. Biol. Chem.* **258,** 7228–7235
51. Firczuk, H., Kannambath, S., Pahle, J., Claydon, A., Beynon, R., Duncan, J., Westerhoff, H., Mendes, P., and McCarthy, J. E. G. (2013) An *in vivo* control map for the eukaryotic mRNA translation machinery. *Mol. Syst. Biol.* **9,** 635